ChemComm

A 25 mA/cm^2 Dye-Sensitized Solar Cell Based on a Near-Infrared-Absorbing Organic Dye and Application of the Device in SSM-DSCs

Journal:	*ChemComm*
Manuscript ID	CC-COM-12-2019-009372.R2
Article Type:	Communication

COMMUNICATION

A 25 mA/cm² Dye-Sensitized Solar Cell Based on a Near-Infrared-Absorbing Organic Dye and Application of the Device in SSM-DSCs

Received 00th January 20xx,
Accepted 00th January 20xx

DOI: 10.1039/x0xx00000x

Hammad Cheema,[a]* Jonathon Watson,[a] Adithya Peddapuram,[a,§] and Jared H. Delcamp[a,*]

A blue organic near infrared (NIR) absorbing sensitizer, AP25, is investigated for use in broadly absorbing dye-sensitized solar cells (DSCs). AP25 shows solar-to-electric conversion with an onset near 900 nm in DSC devices and a photocurrent near 25 mA/cm² when co-sensitized. An all-organic SSM-DSC device reaches 10.3% PCE.

Dye-sensitized solar cells (DSCs) are unique compared to many photovoltaic technologies in terms of attractive aesthetics, indoor/low light applications, and day long performance.[1-3] The sensitizer in DSC devices is critical in controlling photon absorption, electron injection, charge separated lifetimes, and undesired recombination losses.[4, 5] Organic D-π-A sensitizers offer the advantage of modular synthesis, relatively simple purifications, and band gap engineering to tune the light harvesting capabilities.[6] An ideal DSC sensitizer should be able to absorb photons across the visible spectrum and significantly far into the near infrared (NIR) region of the solar spectrum using photons lower in energy than 750 nm efficiently.[7, 8] Additionally, the sensitizer should provide functionality to insulate the photoelectrode (most commonly TiO_2-based) surface from oxidants in the electrolyte as a barrier to interfacial recombination losses.[9-11]

Proaromatic functionality allows for the incorporation of aromatic groups in the excited-state which lowers the energy needed for photoexcitation. Thieno[3,4-b]thiophene (3,4-TT) is a proaromatic π-bridge which can allow NIR photon-to-electric conversion when used in intramolecular charge transfer (ICT) dye designs.[12, 13] When combined with strongly donating triarylamine (TAA) groups and cyanoacrylic acid (CAA) group, we have shown 3,4-TT can absorb photons as low in energy as 700 nm.[14] Introduction of an added thiophene or furan π-bridge between the TAA group and the 3,4-TT group bathochromically shifted the photon absorption onset from 700 nm to 800 nm. Interestingly, these dyes retained favorable energetics for electron transfers within DSC devices upon addition of secondary π-bridge functionality. The **AP25** dye design seeks to further increase the conjugated π-system through the introduction of a cyclopentadithiophene (CPDT) in place of thiophene or furan as the secondary π-bridge (**Fig. 1**). CPDT is chosen due to the literature demonstrating excellent ICT events with this bridge for high molar absorptivities and low energy light absorption. Additionally, CPDT has a convenient position for rapid alkylations resulting in a three-dimensional geometry at the π-bridge for 4,4-bis(2-ethylhexyl)-4H-cyclopenta[2,1-b:3,4-b']dithiophene ($CPDT^{EtHx}$) which can reduce dye-dye aggregation and promote TiO_2 surface protection in multiple directions.[10, 15]

AP25 was synthesized in 4 steps from intermediates known in the literature (Scheme S1).[12, 16] Briefly, 4-bromo-6-formylthieno[3,4-*b*]thiophene-2-carboxylic ester (**1**) was coupled to stannylated $CPDT^{EtHx}$ (**2**) via a Stille coupling to give the linked π-bridge 3,4-TT-$CPDT^{EtHx}$ (**3**) in 71% yield. *N*-bromosuccinimide (NBS) bromination of the CPDT π-bridge, and coupling to bis(hexyloxy)triphenyl amine boronic ester (**5**) gave the TAA-3,4-TT-$CPDT^{EtHx}$ aldehyde in intermediate (**6**) in 44% yield over two steps. Finally, the synthesis of **AP25** was completed after Knoevenagel condensation to afford the target dye in 40% yield.

Absorption spectroscopy and electrochemical measurements were undertaken with **AP25** to access the suitability of **AP25** for DSC devices (Fig. 1, Table 1). **AP25** is observed to have a broad absorption band across the visible and near-infrared region extending from 500 nm to 800 nm in dichloromethane. **AP25** has an absorption maximum (λ_{max}) of 660 nm and an absorption onset (λ_{onset}) of 780 nm found from drawing a tangent line on the low energy side of the absorption spectrum (Fig. S1). This corresponds to a bathochromic shift from 665 nm to 780 nm relative to a prior reported analogue (**PB1**) without the CPDT π-bridge (Fig. S1).[12] The bathochromically shifted absorption spectrum is accompanied by an increase in the molar absorptivity of **AP25** compared to **PB1** (30,000 - –

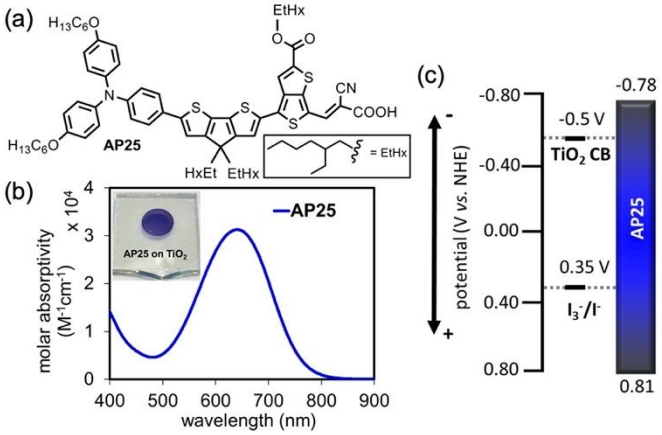

Fig. 1. a) Chemical structure of **AP25** b) UV-Vis absorption of **AP25** (inset shows **AP25** on TiO_2) c) energy level diagram.

[a] 481 Coulter Hall, Chemistry Department, University of Mississippi, University, MS, 38677, USA. Email: hammad.a.cheema@gmail.com; delcamp@olemiss.edu
[b] § Present Address: VolvoChem, Richmond, California 94806, USA.
†Electronic supplementary information (ESI) available: Experimental details about device assembly protocols, electrolyte, and dye adsorption solution preparation. See DOI: 10.1039/x0xx00000x

Table 1. Electronic absorption and electrochemical data for **AP25**.

Dye	λ_{max} (nm)[a]	λ_{onset} (nm)[b]	ε ($M^{-1}cm^{-1}$)[a]	$E_{(S+/S)}$ (V)[c]	$E_{(S+/S^*)}$ (V)[d]	E_g^{opt} (eV)[e]
AP25	660	780	30,000	0.81	-0.78	1.59

[a] Measured in CH_2Cl_2. [b]Onset values taken from the x-intercept of the downward line of best fit on the absorbance curve on the low energy side. [c]Values are reported versus NHE. [d] $E_{(S+/S^*)}$ was calculated from the equation $E_{(S+/S^*)} = E_{(S+/S)} - E_g^{opt}$. [e]Conversion from nanometers to eV was calculated by $E_g^{opt} = 1240/\lambda_{onset}$.

$M^{-1}cm^{-1}$ vs. 26,000 $M^{-1}cm^{-1}$), which suggest the introduction of the CPDT π-bridge enhances ICT across the molecule.[10]

Electrochemical analysis via cyclic voltammetry (Fig. S2) reveals that the bathochromic shift upon addition of the CPDT π-bridge is due an decrease in the ground-state oxidation potential ($E_{(S+/S)}$) of the dye by 280 mV presumably due to the electron rich nature of the CPDT group (0.81 V vs. normal hydrogen electrode (NHE) for **AP25** vs. 1.09 V for **PB1**, Fig. S1, S2).[16, 17] Taking the triiodide/iodide (I_3^-/I^-) redox shuttle at 0.35 V, this allows for a free-energy of regeneration (ΔG_{reg}) of 460 mV.[17, 18] An excited-state oxidation potential ($E_{(S+/S^*)}$) of –0.78 V was found through the equation $E_{(S+/S^*)} = E_{(S+/S)} - E_g^{opt}$, where E_g^{opt} is the optical energy gap found from the onset of the absorption spectrum. This corresponds to a free energy for electron injection (ΔG_{inj}) into the TiO_2 conduction band (CB) of approximately 280 mV when the TiO_2 CB is taken at –0.5 V versus NHE, which is near the minimum driving force needed for fast electron transfer.[18, 19] In terms of thermodynamic electron injection and dye regeneration free energies, **AP25** has minimal free energy losses. In comaprison with well known benchmark sensitizers **N719** and **black dye** (Fig. S1), the adopted design strategy resulted in good energetics with less energy loss due to injection or regenerative overpotentials and an electronic absorption with a higher molar absorptivity (Table S1).[20, 21] Additionally, density functional theory (DFT) caluculations at the B3LYP/6–311G(d,p) level show the HOMO delocalized on the TAA, CPDT, and 3,4-TT (lesser amount) groups (Fig. S3). The LUMO extends from the CAA group to the CPDT group as expected for an ICT system. The HOMO is well possitioned far from the TiO_2 anchor to promote extended charge separation after interfacial charge transfer, and the LUMO is well positioned spatially for efficient charge transfer to TiO_2. Time-dependant (TD)-DFT shows very close agreement with experiment for the vertical transition comparison to λ_{max} (1.86 vs. 1.88 eV) indicating this model is a reasonable approximation of the dye properties (Table S2).

AP25 was tested in DSC devices via current density-voltage (*J-V)* curve and incident photon-to-current conversion efficiency (IPCE) measurements (Table 2, **Fig. 2**). The power conversion efficiency (PCE) was calculated according to the equation $PCE = (J_{sc} \times V_{oc} \times FF)/I_0$ where, J_{sc} is the short-circuit current density, V_{oc} is the open-circuit voltage, FF is the fill factor and I_0 is the intensity of the incident light (1 sun, air mass 1.5G). **AP25** in a single dye DSC device shows a broad IPCE response from 350 nm to near 900 nm (Fig. 2) with a peak IPCE value of 75%. The bathochromic shift in absorption onset on TiO_2 films from 800 nm (Fig. S15b) to 900 nm (Fig. 2) for the IPCE of **AP25** is most likely caused by additives in the electrolyte (Figure S15c).[22] This panchromatic IPCE spectrum corresponds to a high J_{sc} of 19.9 mA/cm^2. Notably, IPCE onsets beyond 850 nm and IPCE peak conversions in excess of 60% have rarely been observed in literature for organic dyes.[17, 23, 24] **AP25** represents a notable step forward with regard to broad IPCE and NIR dyes with a record setting J_{SC} value obtained. In fact, the IPCE breadth and photocurrent output of **AP25** is higher than many well-known broadly absorbing Ru(II) metal sensitizers.[25, 26] A noticeable drop in the IPCE spectrum is present in the 400-550 nm region of **AP25** DSC devices (Fig. 2) due to an inherent lack of photon absorption as observed in the UV-Vis for **AP25** in solution (Fig. 1) and on dye anchoared TiO_2 films (Fig. S15). Thus, co-sensitization with an orange dye (**D35**) with complimentary light absorption in the region of the **AP25** spectrum where a minimum is observed at ~450 nm on TiO_2 can increase photocurrents (Fig. S15).[9, 27-33] An **AP25/D35** DSC device gives a photocurrent of 21.4 mA/cm^2, an 8.0 % overall PCE, and a peak IPCE of 80% with better photon conversion in the 400-550 nm region without loss in conversion at lower energy wavelengths (Table 2, Fig. 2). **AP25** and **D35** synergistically resulting in better surface protection as evidenced by an increased photovoltage for **AP25/D35** DSC devices, larger charge transfer resistance at the dye-TiO_2 interface to the redox shuttle via electrochemical impedance spectroscopy measurements (Fig. S4), and a longer lifetime of electrons in TiO_2 as observed with small modulated photovoltage transient measurements (Table 2, Fig. S4). Addition of a "cyclized transparent optical polymer (CYTOP)" with siloxane end caps (M-type) as an anti-reflective film to the **AP25/D35** DSC device enhanced light transmission through the fluorine-doped tin oxide (FTO) glass electrode for an observed peak photocurrent of 24.5 mA/cm^2, which shows (1) the highest J_{sc} value we are aware of for an organic sensitizer DSC, (2) a higher J_{sc} than well-known precious-metal dyes such as **N719** and **black dye**, (3) one of the

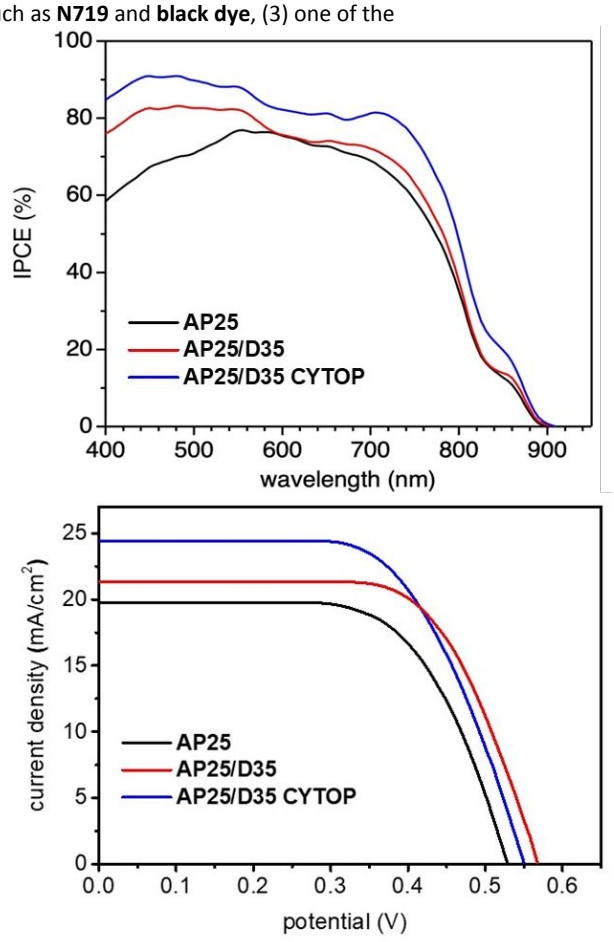

Fig. 2. IPCE curves (top) and *J-V* curves (bottom) for **AP25** and **AP25/D35** DSC devices.

Table 2. Summary of DSCs device data for **AP25** and co-sensitized **AP25/D35** dyes.[a]

Entry	Dye	J_{sc} (mA/cm^2)	J_{sc} (IPCE integrated)	V_{oc} (mV)	FF (%)	PCE (%)	IPCE at 500 nm (%)	Dye Loading (mol/cm^2)[b]
1	**AP25**	19.9	19.0	527	65	6.8	67	4.60 x 10^{-6}
2	**AP25+D35**	21.4	20.8	564	67	8.0	80	2.78 x 10^{-6} /5.96 x 10^{-6}
3	**AP25+D35 CYTOP**	23.7±0.7 (24.5)	23.4	569.5±11 (551)	63±0.5 (63)	8.3±0.2 (8.4)	86	

[a] See the experimental section for device assembly and other details. Values in parenthesis for entry 3 are the highest values observed. [b] Measured with a 2.5 µm thick TiO_2 electrode.

highest known J_{sc} values for any DSC system comparable only to some recent ruthenium and osmium systems, and (4) a higher J_{sc} than that observed from high efficiency perovskite solar cells (Table S7, Fig. S14).[17, 34, 35] Extending electricity production further into the NIR with high J_{sc} values is critical for multijunction systems working in unison with other solar cell technologies, and this ~25 mA/cm^2 device is a significant finding in this direction (further demonstration below). Device optimization strategies, such as chenodeoxycholic acid (CDCA) concentration optimizations led to an enhancement in the J_{sc} (19.9 vs. 17.3 mA/cm^2, max IPCE 75% vs. 65% at 580 nm, Fig. S3-S5) and V_{oc} (527 vs. 473 mV, Table S3) likely due to changing dye-dye surface interactions and slowing recombination losses.[36] Electrochemical impedance spectroscopy (EIS) in the dark and electron lifetime measurements by small modulation photovoltage transient method (SMPVT) results are discussed in supplemental information (Section 6, Fig. S4-S13, Table S3-S6). To further elucidate the role of the individual **D35** and **AP25** dyes in the high performing co-sensitized devices and IPCE profile output, dye loading measurements (Fig. S15 and Table S8) were carried out. Though amount of **D35** was half that of **AP25** in the optimized concentrations for dye dipping solutions (1:2) resulting in high photocurrent DSC devices, **D35** was estimated to be double the amount of **AP25** on the TiO_2 surface which is probably due to the relatively compact molecular size of **D35**. Additionally, preliminary photostability analysis (Fig. S16) of the **AP25**+**D35** device with a UV cutoff filter (>400 nm photons transmitted) shows a functional device for greater than 1000 hours with only a ~20% loss in PCE.

The **AP25**+**D35** DSC device IPCE onset of 895 nm with up to 24.5 mA/cm^2 of photocurrent is attractive for use as a back cell in sequential series multijunction-DSCs (SSM-DSCs, Fig. 3, S17-S19, Table 3).[37, 38] SSM-DSCs are mechanically stacked single illuminated area series connected devices which exploit a photon management strategy in individual subcells by controlling TiO_2 film thickness, order of sensitizer illumination based on absorption breadth, and redox shuttle.[37, 38] SSM-DSCs can lead to higher overall PCE than individual devices if the absorption components are carefully selected to match subcell photocurrents.[39, 40] For a two subcell SSM-DSC device, a top subcell based on **D35** dye and Co(bpy)$_3^{3+/2+}$ redox shuttle was selected due to the IPCE range of 400-650 nm for this device using half of the photons available to a **AP25+D35** subcell (Fig. S20-S23). This translates to a PCE >10 % for a metal-free dye based SSM-DSC device for the first time with V_{oc} output of 1.47 V.[41]

For a three subcell organic dye based SSM-DSC device employing **MK2** (Fig. S20 and Fig. S23, IPCE onset 750 nm) as a middle subcell red dye with a Co(bpy)$_3^{3+/2+}$ redox shuttle. An ~10% PCE was maintained with an increase in photovoltage to 2120 mV (Fig. 3, Table 3, Table S10 and S11). This example highlights the value of the **AP25**+**D35** DSC device since the prior report on two and three subcells systems with **D35** and organic dyes have reached only 7.1%

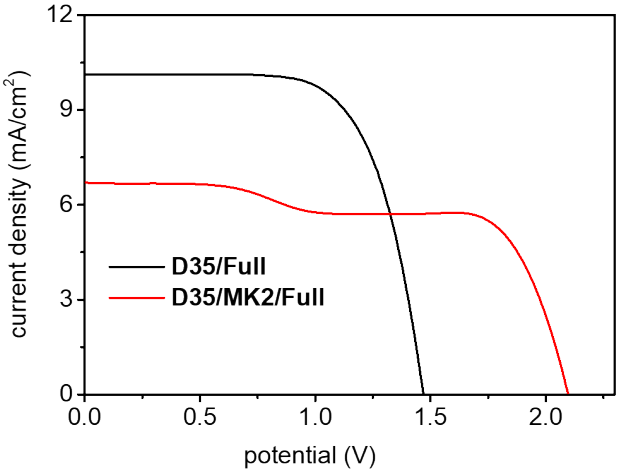

Fig. 3. *J-V* curves of SSM-DSC devices made with all metal-free dyes, "Full" indicated AP25/D35 co-sensitized subcell.

Table 3. Summary of SSM-DSC device data and comparison with previous results.[a]

dye	TiO_2 thickness	J_{sc} (mA/cm^2)	V_{oc} (mV)	*FF* (%)	*PCE*
two-subcell SSM-DSC devices					
D35/(AP25+D35)	5 µm/Full	10.1	1470	71	10.3
D35/Y123[b]	1.5 µm/Full	5.9	1918	62	7.1
Y123/B11[c]	2.2 µm/Full	9.3	1550	60	8.7
three-subcell SSM-DSC devices					
D35/MK2/(AP25+D35)	1.8 µm/3.5 µm/Full	6.8	2120	68	10.1
D35/Y123/Y123[b]	1.2 µm /2.2 µm /Full	3.6	2666	72	7.0
D35/B11/B11[c]	1.5 µm/2.2 µm/Full	5.5	2280	71	9.3

[a] "Full" is an **AP25**+**D35** co-sensitized subcell with 10 or 15 µm of a TiO_2 active layer and 5 µm of TiO_2 scattering layer. Details of individual cells and statistical average from multiple devices is given in the SI (Table S6-S9). [b] Previously reported.[37] [c] Previously reported.[41]

and 7.0% PCE due to absorption breadth limitations of the back subcell. Further, **AP25+D35** ourperforms metal complex sensitizers as the back cell due to its efficient NIR response beyond 750 nm (Table 3, 8.7% and 9.3% PCE compared to 10.3% and 10.1% for two-subcell and three-subcell SSM-DSC devices, respectively).[41] In fact, the AP25/D35 subcell has enabled the fabrication of a precious metal free solar-to-fuel electrolysis system.[42]

A simple to synthesize, blue colored organic sensitizer gave a broad solar-to-electric response with onset at 895 nm in DSC devices. Efficient and panchromatic current generation throughout the IPCE spectrum (350-900 nm) is possible with the use of a dye comprised of a proaromatic (3,4-TT) π-bridge, a highly alkylated TAA donor, and an electron rich CPDT π-bridge. The **AP25** optical and electrochemical properties observed show good energetics for use in DSC devices. An overall power conversion efficiency of 6.8% for **AP25** was improved to 8.4% by co-sensitization with an orange dye and the use of a CYTOP anti-reflective coating. PCE values of >10% were achieved when **AP25+D35** based DSC were used as back subcells in **SSM-DSC** devices with front **D35** subcells. With an aesthetically attractive blue color, **AP25** offers an approach to a highly efficient and broad absorbing organic dye.

Conflicts of interest

There are no conflicts to declare.

Acknowledgments

H.C., J.W., A.P., and J.H.D. thank the National Science Foundation for generous support through the CAREER Award 1455167.

Corresponding Author*

*Hammad Cheema, hammad.a.cheema@gmail.com

*Jared H. Delcamp, delcamp@olemiss.edu

References

1 B. O'Regan and M. Grätzel, *Nature*, 1991, **353**, 737-740.
2 A. Hagfeldt, G. Boschloo, L. Sun, L. Kloo and H. Pettersson, *Chem. Rev.*, 2010, **110**, 6595-6663.
3 A. Fakharuddin, R. Jose, T. M. Brown, F. Fabregat-Santiago and J. Bisquert, *Energy Environ. Sci.*, 2014, **7**, 3952-3981.
4 S. Ardo and G. J. Meyer, *Chem. Soc. Rev.,* 2009, **38**, 115-164.
5 S. Yoon, S. Tak, J. Kim, Y. Jun, K. Kang and J. Park, *Building and Environment*, 2011, **46**, 1899-1904.
6 Y. Wu, W. H. Zhu, S. M. Zakeeruddin and M. Grätzel, *ACS Appl. Mater. Interfaces*, 2015, **7**, 9307-9318.
7 B. E. Hardin, H. J. Snaith and M. D. McGehee, *Nat. Photon.*, 2012, **6**, 162-169.
8 H. Tian, X. Yang, R. Chen, A. Hagfeldt and L. Sun, *Energy Environ. Sci.*, 2009, **2**, 674-677.
9 D. P. Hagberg, X. Jiang, E. Gabrielsson, M. Linder, T. Marinado, T. Brinck, A. Hagfeldt and L. Sun, *J. Mater. Chem.*, 2009, **19**, 7232-7238.
10 R. Li, J. Liu, N. Cai, M. Zhang and P. Wang, *J. Phys. Chem. B*, 2010, **114**, 4461-4464.
11 Z. Yao, H. Wu, Y. Ren, Y. Guo and P. Wang, *Energy Environ. Sci.*, 2015, **8**, 1438-1442.
12 P. Brogdon, F. Giordano, G. A. Puneky, A. Dass, S. M. Zakeeruddin, M. K. Nazeeruddin, M. Grätzel, G. S. Tschumper and J. H. Delcamp, *Chem. Eur. J.*, 2016, **22**, 694-703.
13 P. Brogdon, H. Cheema and J. H. Delcamp, *ChemSusChem*, 2017, **10**, 3624-3631.
14 M. Liang and J. Chen, *Chem. Soc. Rev.*, 2013, **42**, 3453-3488.
15 J. H. Yum, E. Baranoff, F. Kessler, T. Moehl, S. Ahmad, T. Bessho, A. Marchioro, E. Ghadiri, J. E. Moser, C. Yi, M. K. Nazeeruddin and M. Grätzel, *Nat. Commun.*, 2012, **3**, 631.
16 Y. Hu, A. Abate, Y. Cao, A. Ivaturi, S. M. Zakeeruddin, M. Grätzel and N. Robertson, *J. Phys. Chem. C*, 2016, **120**, 15027-15034.
17 P. Brogdon, H. Cheema and J. H. Delcamp, *ChemSusChem*, 2018, **11**, 86-103.
18 G. Boschloo and A. Hagfeldt, *Acc. Chem. Res.*, 2009, **42**, 1819-1826.
19 N. P. Liyanage, A. Yella, M. Nazeeruddin, M. Grätzel and J. H. Delcamp, *ACS Appl. Mater. Interfaces*, 2016, **8**, 5376-5384.
20 M. K. Nazeeruddin, S. M. Zakeeruddin, R. Humphry-Baker, M. Jirousek, P. Liska, N. Vlachopoulos, V. Shklover, C.-H. Fischer and M. Grätzel, *Inorg. Chem.*, 1999, **38**, 6298-6305.
21 P. Péchy, T. Renouard, S. M. Zakeeruddin, R. Humphry-Baker, P. Comte, P. Liska, L. Cevey, E. Costa, V. Shklover, L. Spiccia, G. B. Deacon, C. A. Bignozzi and M. Grätzel, *J. Am. Chem. Soc.*, 2001, **123**, 1613-1624.
22 R. Li, D. Liu, D. Zhou, Y. Shi, Y. Wang and P. Wang *Energy Environ. Sci.*, 2010, **3**, 1765-1772.
23 D. H. Lee, M. J. Lee, H. M. Song, B. J. Song, K. D. Seo, M. Pastore, C. Anselmi, S. Fantacci, F. De Angelis, M. K. Nazeeruddin, M. Gräetzel and H. K. Kim, *Dyes and Pigm.*, 2011, **91**, 192-198.
24 X. Lu, T. Lan, Z. Qin, Z.-S. Wang and G. Zhou, *ACS Appl. Mater. Interfaces*, 2014, **6**, 19308-19317.
25 M. K. Nazeeruddin, F. De Angelis, S. Fantacci, A. Selloni, G. Viscardi, P. Liska, S. Ito, B. Takeru and M. Grätzel, *J. Am. Chem. Soc.*, 2005, **127**, 16835-16847.
26 C. Y. Chen, M. Wang, J. Y. Li, N. Pootrakulchote, L. Alibabaei, C. H. Ngoc-le, J. D. Decoppet, J. H. Tsai, C. Grätzel, C. G. Wu, S. M. Zakeeruddin and M. Grätzel, *ACS Nano*, 2009, **3**, 3103-3109.
27 J. H. Yum, T. W. Holcombe, Y. Kim, J. Yoon, K. Rakstys, M. K. Nazeeruddin and M. Grätzel, *Chem. Commun.*, 2012, **48**, 10727-10729.
28 K. Pei, Y. Wu, H. Li, Z. Geng, H. Tian and W.-H. Zhu, *ACS Appl. Mater. Interfaces*, 2015, **7**, 5296-5304.
29 A. Peddapuram, H. Cheema, R. E. Adams, R. H. Schmehl and J. H. Delcamp, *J. Phys. Chem. C*, 2017, **121**, 8770-8780.
30 D. Kuang, P. Walter, F. Nüesch, S. Kim, J. Ko, P. Comte, S. M. Zakeeruddin, M. K. Nazeeruddin and M. Grätzel, *Langmuir*, 2007, **23**, 10906-10909.
31 C. Magne, M. Urien and T. Pauporté, *RSC Adv.*, 2013, **3**, 6315-6318.
32 W. Zhang, W. Li, Y. Wu, J. Liu, X. Song, H. Tian and W.-H. Zhu, *ACS Sustain. Chem. Eng.*, 2016, **4**, 3567-3574.
33 J. M. Cole, G. Pepe, O. K. Al Bahri and C. B. Cooper, *Chem. Rev.*, 2019, **119**, 7279-327.
34 K. Rakstys, M. Saliba, P. Gao, P. Gratia, E. Kamarauskas, S. Paek, V. Jankauskas and M. K. Nazeeruddin, *Angew. Chem.*, 2016, **55**, 7464-7468.
35 N. Pellet, P. Gao, G. Gregori, T. Y. Yang, M. K. Nazeeruddin, J. Maier and M. Grätzel, *Angew. Chem.*, 2014, **53**, 3151-3157.
36 N. R. Neale, N. Kopidakis, d. L. van, M. Grätzel and A. J. Frank, J. Phys. Chem. B, 2005, 109, 23183-23189.
37 H. Cheema, R. R. Rodrigues and J. H. Delcamp, *Energy Environ. Sci.*, 2017, **10**, 1764-1769.
38 R. R. Rodrigues, H. Cheema and J. H. Delcamp, *Angew. Chem.*, 2018, **57**, 5472-5476.
39 T. Kinoshita, J. T. Dy, S. Uchida, T. Kubo and H. Segawa, *Nat Photon*, 2013, **7**, 535-539.
40 T. Yamaguchi, Y. Uchida, S. Agatsuma and H. Arakawa, *Sol. Energy Mater. Sol. Cells*, 2009, **93**, 733-736.
41 H. Cheema and J. H. Delcamp, *Adv. Energy Mater.*, 2019, **9**, 1900162.
42 H. Cheema, J. Watson, P. S. Shinde, R. R. Rodrigues, S. Pan and J. H. Delcamp, *Chem. Commun.*, 2020, **DOI**: 10.1039/C9CC09209A.

COMMUNICATION

TOC Graphic: